

# Refractory-metal stabilized amorphous stainless steel

## Part 1 *Formation and stability of amorphous stainless steel with W or Ti*

RONG WANG

*Pacific Northwest Laboratory\*, Richland, Washington 99352, USA*

Commercial stainless steel alloys have been made into amorphous, or glassy, states by adding nearly 10 at % of refractory metals, such as W or Ti, via high-rate sputter deposition. The formation of these stable amorphous stainless steel alloys required alloy compositions beyond the equilibrium bcc solid solution phase field. For the amorphous alloys containing W, the crystallization temperature increased from 760 to 1035 K as the W content was increased from 11 at % W to 23 at % W. The high crystallization temperatures were attributed to the high resistance to crystallization of the complex intermediate  $\chi$  and  $\mu$  phases, which occurred at 11 and 23 at % W respectively.

### 1. Introduction

In recent years, a large number of iron–chromium-based amorphous, or glassy, alloys have been obtained by rapid quenching from the liquid state. These amorphous alloys are the “metal–metalloid” (M–Md) type alloys containing one or more metalloid elements, such as P, B, C, or Si and have compositions near a general formula of  $(\text{Fe, Ni, Cr})_{80}\text{Md}_{20}$ , where Md represents either a single or several metalloid elements. The unique amorphous structure has exhibited high mechanical strength [1–3] and improved corrosion resistance [4–6]. However, due to the large quantity of metalloid elements, compositions of these types of amorphous alloys are quite different from commercial engineering materials such as steels and stainless steels. In most cases, the amorphous alloys have low thermal stability with crystallization temperatures below 800 K [7]. Rapid quenching techniques have been applied to several engineering materials like stainless steels [8, 9], and high-speed steels [10], but no amorphous phase was obtained. The author found only one reported case of amorphous steel, a commercial 304 stainless steel that was made by sputter deposition in thin film form [11]. Since the amorphous film was extremely thin, about 200 nm, the structure and properties of this film were not reported.

We have used a high-rate sputter deposition technique to render commercial stainless steel alloys containing a small quantity of refractory metal such as W or Ti into an amorphous state. These alloys are the “metal–metal” (M–M) type alloys based on transition metals. The amorphous stainless steel alloys were formed as coatings with thicknesses from 300  $\mu\text{m}$  to several millimeters. This is thicker than any reported metal–metal amorphous alloys and thus many structure–property relationships could be studied. This paper is one of a series that report on the investigation of the unique formation, structure, and properties of the refractory-metal stabilized amorphous stainless steel alloys and a comparison of these properties of those crystalline stainless steel alloys.

### 2. Experimental procedure

The amorphous alloys were prepared by a d.c. triode, high-rate sputter deposition technique described elsewhere [12]. Sputtering targets were fabricated by embedding several 0.625 cm diameter rods of the refractory metal, either W or Ti, in a 7.62 cm diameter ASIS 304 stainless steel disc of about 1 cm thickness. The number of rods and their positions was varied to obtain deposits either with uniform or graded composition. The

\*Operated for the Department of Energy by Battelle Memorial Institute under contract number DE-AC06-76-RLO 1830.

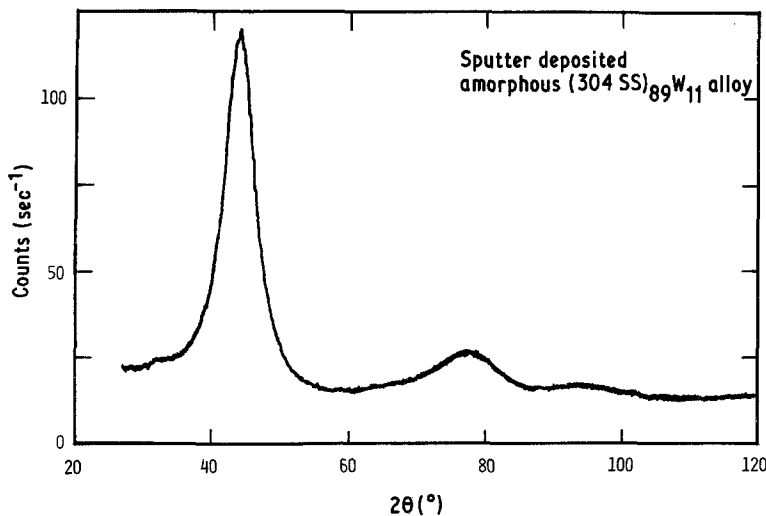


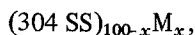
Figure 1 X-ray diffraction pattern for the amorphous  $(304\text{ SS})_{89}\text{W}_{11}$  alloy, typical of the patterns observed for  $(304\text{ SS})_{100-x}\text{M}_x$ ,  $11 \leq x \leq 54$  where  $x$  is at % W or Ti.

substrate was a 6.35 cm diameter by 0.625 cm thick copper disc welded to a stainless steel stem. This arrangement permitted temperature control by cooling external to the vacuum on the back side of the substrate. The substrate was either cooled to liquid nitrogen temperature,  $-195^\circ\text{C}$ , or water-cooled to maintain the temperature at 20 to  $25^\circ\text{C}$  during the deposition run. High-purity krypton sputtering gas was admitted to the chamber after the system was baked for 12 h to reach a pressure of  $1 \times 10^{-8}$  torr. For a typical deposit, a plasma potential of  $-40\text{ V(d.c.)}$  at a plasma current of 3.5 A was used. The typical deposits were about  $300\ \mu\text{m}$  thick and were produced at approximately  $25\ \mu\text{m h}^{-1}$  deposition rate.

The composition of the deposit was analysed by energy dispersive X-ray analysis (EDAX) in a scanning electron microscope. The deposits were examined by X-ray diffraction and transmission electron microscopy for identification of the glassy structure and the crystalline phases. Crystallization temperatures were derived from both differential scanning calorimetry (DSC) measurement at a scanning rate of  $20\ \text{K min}^{-1}$  and isothermal annealing in a vacuum for 1 h. Hardness measurements were made with a Zeiss microhardness tester.

### 3. Results

The amorphous alloys, prepared with a starting material of AISI 304 stainless steel (304 SS), and refractory metal inserts had a wide composition range which could be expressed by the formula



where M is a refractory metal, either W or Ti, and  $x$  is the atomic per cent. A number of amorphous stainless steel alloys containing W were prepared at both  $-195^\circ\text{C}$  and  $25^\circ\text{C}$  with  $x = 11, 12, 14, 21, 23$  and 54. The diffraction pattern of the amorphous alloys showed a broad first diffraction peak of half-peak width about  $5^\circ (2\theta)$ , followed by weak second and third diffraction peaks, see Fig. 1. Both X-ray diffraction and transmission electron microscopy studies indicated that the amorphous stainless steel alloys had an amorphous structure similar to that of the metal-metal amorphous W-Fe [13] and Mo-Co [14] alloys reported previously. The hardness of the amorphous alloys, was observed to increase with increase in W content, see Fig. 2.

For the amorphous alloys containing Ti, a deposit was prepared with a graded composition between  $x = 3.6$  and 9.5 at % in order to determine the composition range that separated the crystalline and amorphous phases, see Fig. 3a. An amorphous phase was formed for  $x$  equal to or greater than 8 at % and the crystalline phase with  $x$  equal to or less than 7 at %. The crystalline phase had the bcc structure of sputter-deposited 304 and 304 L stainless steel alloys [8, 9]. Between  $x = 7$  and 8 at %, the deposit had mixed amorphous and crystalline phases. The crystalline phase in the amorphous-crystalline mixture region contained many large bcc grains; these large grains were not found in the solely crystalline alloys. The transition from a completely crystalline phase field up to a completely amorphous phase field was therefore separated by only 1 at % Ti. The hardness of the sputter deposited alloys decreased with decreasing Ti content, see Fig. 3b.

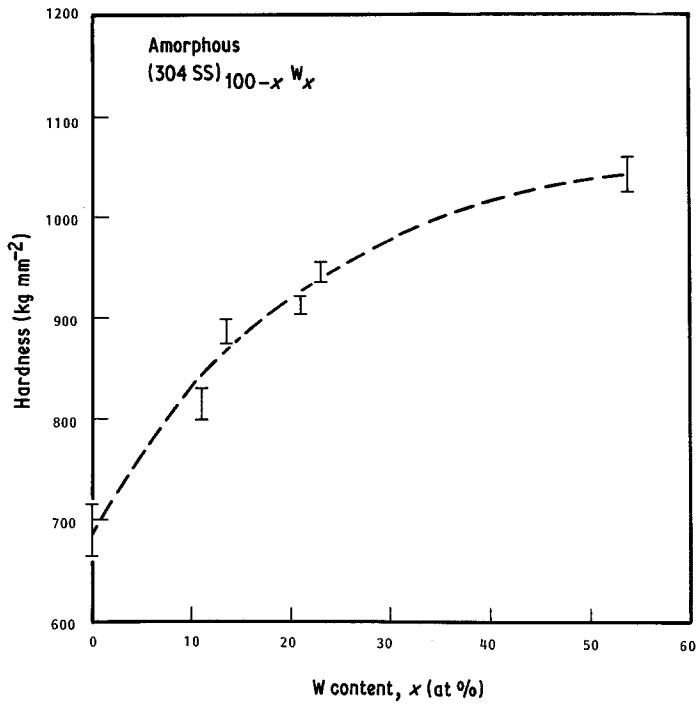


Figure 2 Hardness of the amorphous (304 SS)<sub>100-x</sub>W<sub>x</sub> alloys as a function of x.

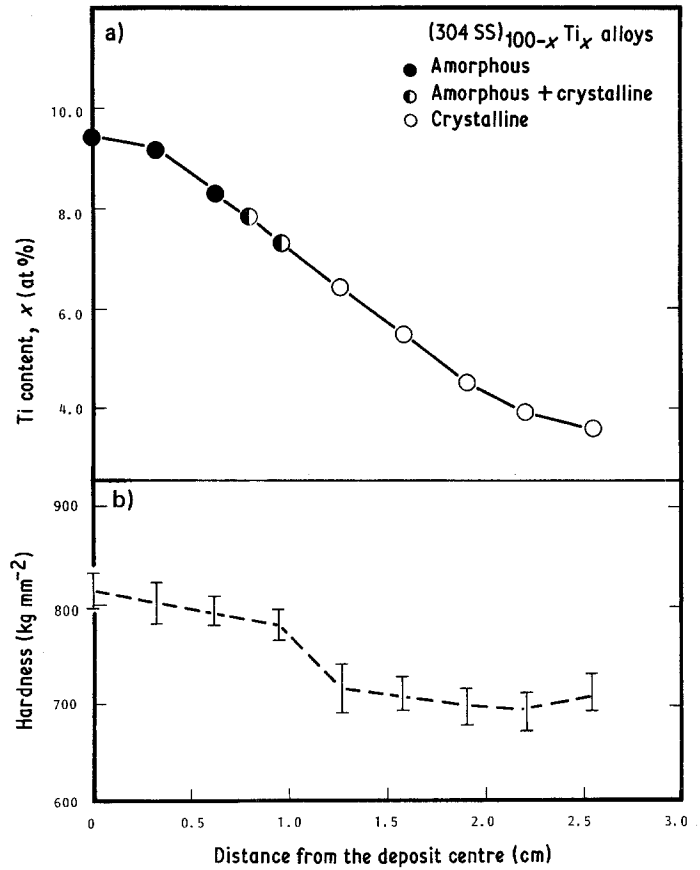


Figure 3 (a) Composition and (b) hardness of a graded (304 SS)<sub>100-x</sub>Ti<sub>x</sub> deposit showing occurrence of amorphous, amorphous and crystalline and crystalline phases.

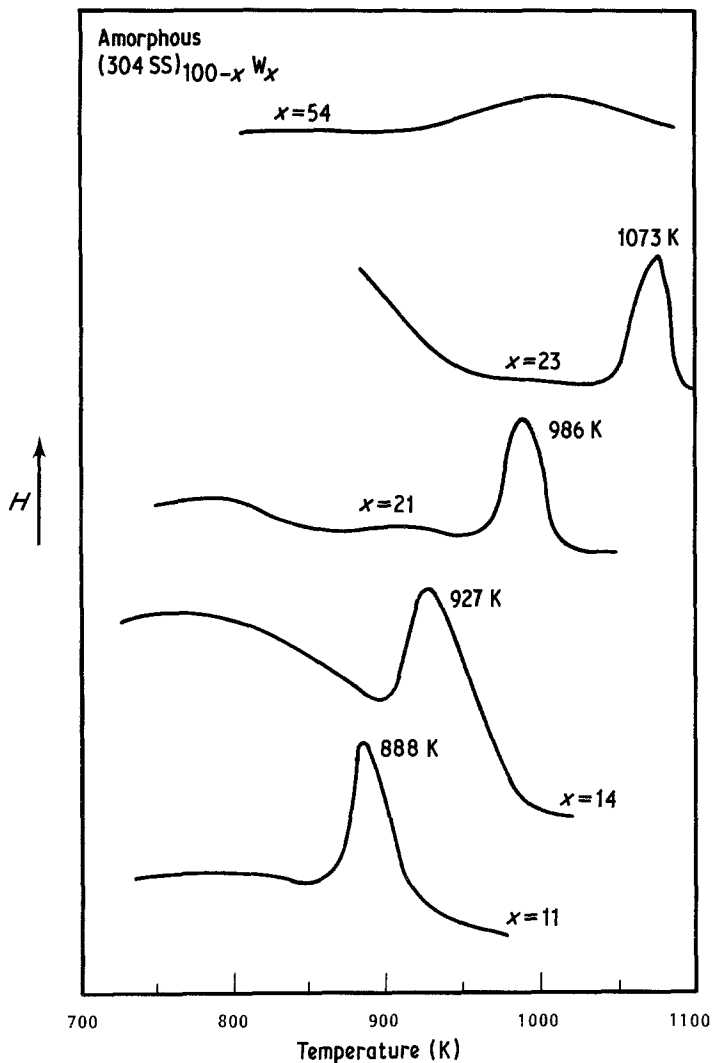


Figure 4 DSC curves for the crystallization temperatures,  $T_{x(\text{DSC})}$ , of the  $(304 \text{ SS})_{100-x}\text{W}_x$  alloys using scanning rate of  $20 \text{ K min}^{-1}$ .

The thermal stability, in terms of the crystallization temperature,  $T_{x(\text{DSC})}$ , derived from DSC measurements increased with W content in the amorphous alloys, as shown in Fig. 4. No DSC peak corresponding to a glass transition temperature,  $T_g$ , was observed. The results of isothermal annealing of the amorphous alloys between 773 and 1173 K in 100 K intervals are shown in Table I. The DSC-derived crystallization temperatures,  $T_{x(\text{DSC})}$  are plotted as a function of the W content in Fig. 5, and compared with those estimated from the isothermal annealing experiments,  $T_{x(\text{ISO})}$ .  $T_{x(\text{DSC})}$  were always higher than  $T_{x(\text{ISO})}$  and the difference was about 130 K for  $x = 11$  at %. The difference reduced rapidly to about 30 K for  $x = 21$  and 23 at %. No thermal peak was observed for alloy  $x = 54$  at % by DSC measurement and a  $T_{x(\text{ISO})}$  was estimated from the isothermal experiment.

Only four types of equilibrium phases were observed from the isothermal annealing experiments, namely a solid solution Fe-rich bcc phase, a W-rich bcc phase, the  $\chi$  phase and the  $\mu$  phase. The Fe-rich bcc phase was observed at  $x$  between 11 and 14 at % along with the amorphous or  $\chi$  phases. The  $\chi$  phase was observed also at  $x$  between 11 and 14 at %; but at 973 K, the crystallized phase was almost 100%  $\chi$  phase. The  $\mu$  phase was observed at  $x$  between 21 and 23 at % at 1073 K. It coexisted with the  $\chi$  phase at  $x = 21$  at % whereas at  $x = 23$  at % it was nearly 100%  $\mu$  phase. At  $x = 54$  at %, the crystalline phase was mainly the W-rich bcc phase with a small amount of the  $\mu$  phase. The crystallization temperature increased rapidly in the composite range of  $x = 11$  to 23 at % and then leveled off at  $x = 54$  at %.

TABLE I Crystallization behaviour of amorphous  $(304\text{ SS})_{100-x}\text{W}_x$  alloys

Composition $x$ (at%)	Crystallization temperature		Phase(s) formed by isothermal annealing for 1 h at				
	$T_x(\text{DSC})$	$T_x(\text{ISO})^*$	773 K	873 K	973 K	1073 K	1173 K
	0	-	-	bcc	fcc	fcc	-
11	888	760	{ bcc (40) <sup>†</sup> am <sup>‡</sup> (60)	{ bcc (40) χ (60)	{ bcc (20) χ (80)	-	-
14	927	830	am	{ bcc (50) χ (50)	{ bcc (5) χ (95)	-	-
21	986	960	am	am	{ χ (30) am (70)	{ χ (20) μ (80)	-
23	1073	1035	am	am	am	μ (100)	μ (100)
54	-	1040	am	am	am	{ bcc (90) am (10)	{ bcc (90) χ (10)

\* $T_x(\text{ISO})$  was estimated based on the fraction of the first crystallized phase.

<sup>†</sup>Number in parentheses indicates approximate per cent of each phase.

<sup>‡</sup>am = amorphous.

## 4. Discussion

### 4.1. Formation and phase stability

Both a high quenching rate and a small quantity of refractory metal addition are needed to stabilize an amorphous alloy made from a crystalline stainless steel alloy. A high quenching rate alone cannot result in a stable amorphous alloy. For example, high-rate sputter deposition of both 304 and 304 L [8, 9] stainless steel at  $-195^\circ\text{C}$

and room temperature produced only a crystalline phase. Apparently, in addition to the high quenching rate, a critical quantity of the refractory metal is needed to stabilize the amorphous stainless steel alloys at or above room temperature.

The quantity of the refractory metal required for the stabilization of the amorphous structure must at least be sufficient to push the crystalline phase boundary for the stainless steel alloys beyond

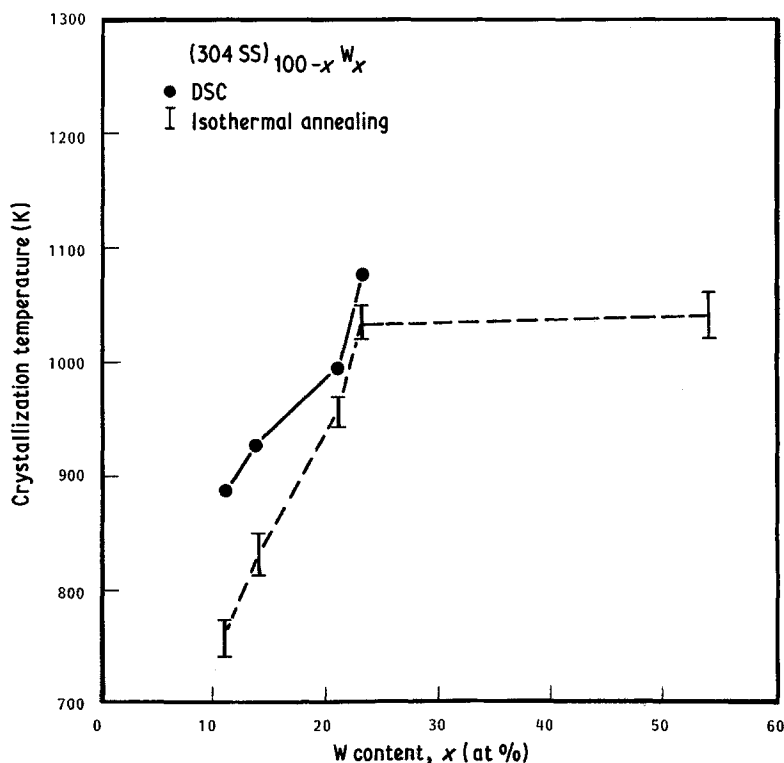


Figure 5 Comparison of the crystallization temperatures of amorphous  $(304\text{ SS})_{100-x}\text{W}_x$  alloys determined by DSC and isothermal annealing measurements.

the solid solution bcc phase field. The thermal stability of the amorphous phases formed in the equilibrium phase fields of bcc, fcc and hcp is very low and usually shows a low crystallization temperature about 10% of the melting temperature [15]. Thus, amorphous alloys formed in the bcc phase field would have a crystallization temperature around 180 K. Consequently, stable amorphous alloys result only at those compositions where crystallization produces a two-phase or multiple phase mixture containing at least one intermediate phase with a complex structure such as a  $\chi$  or a  $\mu$  phase [15].

The reasoning that a critical quantity of W or Ti is required to make amorphous stainless steel alloys can be extended to other refractory metals such as Nb, Ta, Zr, Hf and Mo. Since the solubility of all these metals except Mo is less than 10 at % in iron [16–18], it is likely that the amorphous state in stainless steels can be achieved by alloying with approximately 10 at % of Nb, Ta, Zr, and Hf. Even if the solubility of Mo in iron was as high as 26 at % [19–21], it probably will also take about 10 at % of Mo to achieve the same result because the formation of the  $\chi$  phase  $\text{Cr}_{12}\text{Fe}_{36}\text{Mo}_{10}$  [22] is in the same composition range for the  $\chi$  phases of  $\text{Cr}_{15}\text{Fe}_{34}\text{Ti}_9$  [23] and  $\text{Cr}_{13}\text{Fe}_{35}\text{Ni}_3\text{Ti}_7$  [24]. The formation of the Ti-stabilized amorphous stainless steels with 8 at % of Ti was attributed to these latter phases.

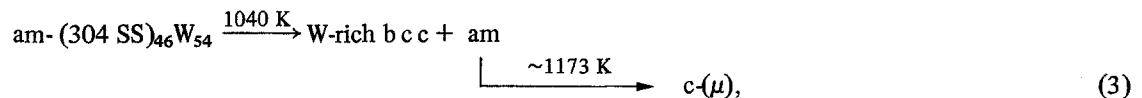
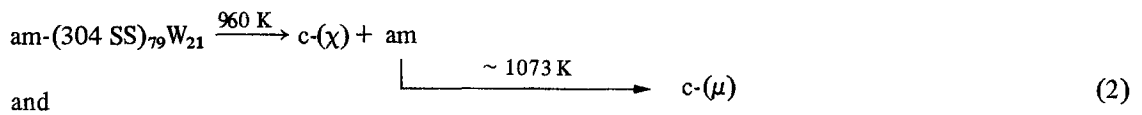
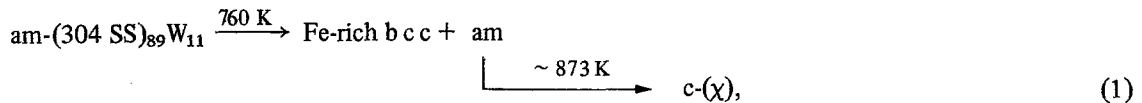
#### 4.2. Crystallization process

The crystallization process of the amorphous stainless steel alloys, analysed from both the DSC measurement and the isothermal annealing experiments showed that the occurrence of the crystalline phase during crystallization proceeds from the bcc, the  $\chi$  and the  $\mu$  phases. The crystallization process, summarized from the isothermal annealing experiments, was the following

where am denotes amorphous and c denotes crystalline. After the first stage of crystallization, the remaining amorphous phase subsequently crystallized in either the  $\mu$  or  $\chi$  phase at a temperature about 100 K higher than that of the bcc phases.

However, the DSC measurements did not show these two stages of crystallization process. Not only did all the DSC measurements show just a single thermal peak for  $x = 11$  to 23 at % but no thermal peak at all was observed for  $x = 54$  at %. Since the  $\text{am-(304 SS)}_{46}\text{W}_{54}$  crystallized mostly into the W-rich bcc phase, the failure to detect the amorphous to bcc phase transition by the DSC measurement was due to the wide temperature range for the nucleation and growth of the bcc crystallites from the amorphous phase [25]. In this case, the DSC measurement was not able to detect the first stage crystallization of the bcc phase. This conclusion is consistent with the observation that  $T_{x(\text{DSC})}$  of the amorphous alloy with  $x = 11$  at % was about 130 K higher than  $T_{x(\text{ASO})}$  where the DSC thermal peak was mostly due to the crystallization of the  $\chi$  phase which is approximately 100 K higher than the bcc phase. The crystallization temperatures for the W-stabilized amorphous stainless steel alloys therefore are better described by  $T_{x(\text{ASO})}$ .

The high thermal stability of the amorphous stainless steel alloys can be related to both the increase of the melting temperature of the alloy with increase in the W content and to the ability of W or Ti to form the complex  $\chi$  and  $\mu$  phases. The crystallization temperatures derived from both DSC and isothermal annealing experiments showed two abrupt increases associated with the occurrence of these two intermediate phases. The first abrupt increase of the crystallization temperature occurred at about 10 to 11 at % W where the amorphous stainless steel was stabilized due to the presence of the  $\chi$  phase upon



crystallization. The second abrupt increase was in the range of 21 to 23 at % W where the  $\mu$  phase occurred upon crystallization.

The increasing crystallization temperature for the bcc phase is therefore attributed to the increase in melting temperature of the bcc phase with increasing W content. For the amorphous alloy of 54 at % W, the crystallization temperature  $T_{x(DSO)}$  for the W-rich bcc phase was about 1040 K, or 210 K higher than for the Fe-rich bcc phase observed at 14 at % W alloy and nearly 300 K higher than for the bcc phase of 11 at % W alloy. Otherwise the abrupt increase of the thermal stability of the amorphous stainless steels over a narrow composition range can be attributed to the increasing difficulty of crystallization of the intermediate phases with complex crystal structures. For comparison, an amorphous alloy at the composition of the  $\chi$  phase in  $Cr_{15}Fe_{34}Ti_9$  was prepared and the DSC measurement indicated a  $T_{x(DSC)}$  of 921 K. This was essentially the same as the  $T_{x(DSC)}$  value of 922 K for the amorphous stainless steel alloys containing 14 at % W.

## 5. Conclusions

Commercial AISI 304 stainless steel alloys were rendered into the amorphous state by incorporating at least 10 at % of W or Ti through high rate sputter deposition. Formation of the amorphous phase requires a critical quantity of W or Ti to bring the alloy composition beyond the crystalline bcc terminal solid solution field. Other refractory metals such as Nb, Ta, Zr, Hf and Mo in similar quantities are also predicted to induce stainless steel amorphous phase formation. The W-stabilized alloys have a high crystallization temperature ranging from 760 to 1040 K. The increase in crystallization temperature was related to both the increase of the melting temperature of the alloys and to the increasing difficulty of crystallizing the intermediate  $\chi$ - and  $\mu$ -type phases which have complex crystal structures.

## Acknowledgements

The author is grateful to J. L. Brimhall, H. E. Kissinger and M. D. Merz for their discussion of the results and to H. E. Kjarmo, A. G. Graybeal and G. L. Robinson for preparing the samples and carrying out X-ray diffraction and hardness measurements. This work was conducted for the Office of Basic Energy Sciences, Division of

Materials Sciences, U.S. Department of Energy under contract DE-AC06-76-RLO 1830.

## References

1. T. MASUMOTO and R. MADDIN, *Acta Metal.* **19** (1971) 725.
2. J. J. GILMAN, *J. Appl. Phys.* **46** (1975) 1629.
3. M. NAKA, K. HASHIMOTO and T. MASUMOTO, *Corrosion* **32** (1976) 146.
4. T. MASUMOTO and K. HASHIMOTO, *Ann. Rev. Mater. Sci.* **8** (1978) 215.
5. K. HASHIMOTO and T. MASUMOTO, in "Rapidly Quenched Metals" edited by N. J. Grant and B. C. Giessen (MIT Press, Mass., 1975) p. 285.
6. T. M. DEVINE, *J. Electrochem. Soc.* **124** (1977) 38.
7. M. NAKA, K. HASHIMOTO and T. MASUMOTO, *Corrosion Eng.* **36** (1980) 679.
8. S. D. DAHLGREN, *Met. Trans.* **1** (1970) 3095.
9. M. D. MERZ, private communications (1980).
10. J. NIEWIAROWSKI and H. MATYJA, in "Rapidly Quenched Metals III" Vol. 1 (The Metals Society, London, 1978) p. 193.
11. P. J. GRUNDY and J. M. MARSH, *J. Mater. Sci.* **13** (1978) 677.
12. S. D. DAHLGREN, in "Rapidly Quenched Metals III" Vol. 2 (The Metals Society, London, 1978) p. 36.
13. R. WANG, M. D. MERZ, J. L. BRIMHALL and S. D. DAHLGREN, in "Rapidly Quenched Metals III" Vol. 1 (The Metals Society, London, 1978) p. 420.
14. R. WANG, M. D. MERZ and J. L. BRIMHALL, *Script. Metal.* **12** (1978) 1037.
15. R. WANG, in "Theory of Alloy Phase Formation" edited by L. H. Bennett (American Institute of Mechanical Engineers, Conference Proceedings of The Metallurgical Society of AIME, 1980) p. 472.
16. M. HANSEN, "Constitution of Binary Alloys" (McGraw Hill Book Co., New York, 1958).
17. R. P. ELLIOT, "Constitution of Binary Alloys, First Supplement" (McGraw Hill Book Co, New York, 1965).
18. W. B. PEARSON, "A Handbook of Lattice Spacings and Structures of Metals and Alloys" (Pergamon Press, Oxford, 1958).
19. W. P. SYKES, *Trans. ASST* **10** (1926) 839.
20. *Idem. Ibid.* **10** (1926) 1035.
21. T. TAKAI and T. MURAKAMI, *ibid.* **16** (1929) 339.
22. J. G. MCMULLIN, S. F. REITER and D. G. EBELING, *Trans. Amer. Soc. Metal.* **46** (1954) 799.
23. N. G. BORISKINA and I. I. KORNILOV, *Zh. Neorg. Khim.* **4** (1959) 2171.
24. H. HUGHES and D. T. LLEWELYN, *J. Iron Steel Inst. (London)* **192** (1959) 170.
25. J. L. BRIMHALL, L. A. CHARLOT and H. E. KISSINGER, *J. Mater. Sci.* **17** (1982) 1149.

Received 27 July  
and accepted 19 September 1981